Molecular Biology of the Cell
Vol. 14, 836–847, March 2003

Sac3 Is an mRNA Export Factor That Localizes to Cytoplasmic Fibrils of Nuclear Pore Complex

Elissa P. Lei,* Charlene A. Stern,* Birthe Fahrenkrog,† Heike Krebber,*‡ Terence I. Moy,*§ Ueli Aebi,† and Pamela A. Silver*‖

*Department of Biological Chemistry and Molecular Pharmacology, Harvard Medical School and Dana Farber Cancer Institute, Boston, Massachusetts 02115; and †M.E. Müller Institute for Structural Biology, Biozentrum, University of Basel, 4056 Basel, Switzerland

Submitted August 19, 2002; Revised October 23, 2002; Accepted October 31, 2002
Monitoring Editor: Joseph Gall

In eukaryotes, mRNAs are transcribed in the nucleus and exported to the cytoplasm for translation to occur. Messenger RNAs complexed with proteins referred to as ribonucleoparticles are recognized for nuclear export in part by association with Mex67, a key *Saccharomyces cerevisiae* mRNA export factor and homolog of human TAP/NXF1. Mex67, along with its cofactor Mtr2, is thought to promote ribonucleoparticle translocation by interacting directly with components of the nuclear pore complex (NPC). Herein, we show that the nuclear pore-associated protein Sac3 functions in mRNA export. Using a mutant allele of *MTR2* as a starting point, we have identified a mutation in *SAC3* in a screen for synthetic lethal interactors. Loss of function of *SAC3* causes a strong nuclear accumulation of mRNA and synthetic lethality with a number of mRNA export mutants. Furthermore, Sac3 can be coimmunoprecipitated with Mex67, Mtr2, and other factors involved in mRNA export. Immunoelectron microscopy analysis shows that Sac3 localizes exclusively to cytoplasmic fibrils of the NPC. Finally, Mex67 accumulates at the nuclear rim when *SAC3* is mutated, suggesting that Sac3 functions in Mex67 translocation through the NPC.

INTRODUCTION

Nuclear export of mRNA in eukaryotes is an obligatory feature of normal gene expression. This process can be divided into two basic steps: formation of the export competent ribonucleoparticle (RNP) and translocation of the RNP through the nuclear pore complex (NPC). Beginning at transcription, mRNAs are bound and packaged by RNA binding proteins to form RNPs (reviewed in Lei and Silver, 2002). Once properly formed, the RNP is actively exported across the nuclear envelope via large aqueous channels formed by the proteinaceous NPC.

Structural integrity of the RNP is an important factor in obtaining export competence. Central to this process is the heterogeneous nuclear (hn)RNP protein Npl3, which is a highly abundant poly $(A)^+$ RNA binding protein in *Saccharomyces cerevisiae* (Wilson *et al.*, 1994). Npl3 shuttles between the nucleus and cytoplasm and is required for nuclear export of mRNA (Flach *et al.*, 1994; Singleton *et al.*, 1995; Lee *et al.*, 1996). The nuclear export of Npl3 is closely tied to that of mRNA, making its localization a useful reporter for mRNA export (Krebber *et al.*, 1999).

The overall structure of the NPC is a central framework with eightfold symmetry embedded in the membrane of the nuclear envelope. In addition, the NPC includes a nuclear-oriented basket of filaments flanked by nuclear and terminal rings as well as fibrils extending into the cytoplasm (reviewed in Stoffler *et al.*, 1999). The NPC is composed of proteins called nucleoporins, many of which are characterized by stretches of FG (Phe-Gly) dipeptide repeats. These FG repeats are thought to serve as binding sites for soluble transport receptors during translocation (Iovine *et al.*, 1995; Radu *et al.*, 1995).

Translocation of RNPs through the NPC is thought to be mediated by the mRNA export factor Mex67 in *S. cerevisiae* or TAP/NXF1 in humans. Together as a heterodimer with its counterpart yeast Mtr2 or metazoan p15, Mex67/TAP is essential for the export of all mRNAs tested in *S. cerevisiae* and *Drosophila* (Hurt *et al.*, 2000; Herold *et al.*, 2001). Mex67/TAP is thought to be recruited to RNPs via interaction with the conserved mRNA export factor yeast Yra1 or human Aly/REF (Sträβer and Hurt, 2000; Stutz *et al.*, 2000; Zenk-

Article published online ahead of print. Mol. Biol. Cell 10.1091/mbc.E02–08–0520. Article and publication date are at www.molbiolcell.org/cgi/doi/10.1091/mbc.E02-08-0520.

Present addresses: ‡Philipps-University Marburg, Institute for Molecular Biology and Tumor Research, Emil-Mannkopff-Straβe 2, 35033 Marburg, Germany; §Department of Genetics, Harvard Medical School and Massachusetts General Hospital, Boston, MA 02114.
‖ Corresponding author. E-mail address: pamela_silver@dfci.harvard.edu.

lusen *et al.*, 2001). Once bound, Mex67/TAP may promote translocation through the NPC through serial interactions with the FG repeats of nucleoporins (Bachi *et al.*, 2000; Sträβer *et al.*, 2000; Strawn *et al.*, 2001).

Mtr2 is required for proper nuclear pore targeting of Mex67. Mutation of *MTR2* causes mislocalization of Mex67 from the nuclear rim to the cytoplasm, and Mtr2 itself interacts with the nucleoporin Nup85 (Santos-Rosa *et al.*, 1998). However, there is disagreement as to whether Mtr2 promotes Mex67 interaction with nucleoporins (Sträβer *et al.*, 2000; Strawn *et al.*, 2001). In higher eukaryotes, the TAP cofactor p15 seems to be important for NPC targeting of TAP (Fribourg *et al.*, 2001; Levesque *et al.*, 2001; Wiegand *et al.*, 2002). The function of these mRNA export receptor heterodimers is conserved because *MEX67/MTR2* can be replaced by introduction of both TAP and p15 in *S. cerevisiae*, although Mtr2 and p15 share no sequence homology (Katahira *et al.*, 1999). Additionally, Mtr2 has been implicated in the export of the large ribosomal subunit (Stage-Zimmermann *et al.*, 2000; Baβler *et al.*, 2001). Moreover, Baβler *et al.* (2001) described a mutant allele of *MTR2* that displays a defect in ribosome but not mRNA export, suggesting that the functions of Mtr2 in both processes are distinct and separable.

An additional requirement for mRNA export is the integrity of the NPC. Three nucleoporin subcomplexes seem to be specifically required for mRNA export, the Nup84-Nup85-Nup120-Nup145-Seh1-secs13 complex, the Nsp1-Nup82-Nup159 complex, and the Nup116-Gle2 complex (Wente and Blobel, 1993; Murphy *et al.*, 1996; Siniossoglou *et al.*, 1996; Teixeira *et al.*, 1997; Bailer *et al.*, 1998; Belgareh *et al.*, 1998; Hurwitz *et al.*, 1998). These nucleoporins may provide docking sites for Mex67 during RNP translocation. In fact, Nup116 can be coimmunoprecipitated with Mex67 from cell lysates (Strawn *et al.*, 2001), and Mex67 is able to bind to fragments containing the FG repeats of Nsp1, Nup116, Nup159, and Rip1 in vitro (Sträβer *et al.*, 2000; Strawn *et al.*, 2001). These interactions are likely to be important for Mex67-mediated RNP translocation through the NPC.

On the cytoplasmic face of the NPC exists a putative complex of proteins that is proposed to serve as the terminal docking site for RNPs. This complex consists of Nup159/Rat7, Gle1, Rip1, and Dbp5/Rat8. Nup159 localizes exclusively to the cytoplasmic fibrils of the NPC, whereas Gle1, Rip1, and Dbp5 display a wider spatial distribution, including the cytoplasmic fibrils (Kraemer *et al.*, 1995; Schmitt *et al.*, 1999; Strahm *et al.*, 1999). Dbp5 is an RNA helicase that has been postulated to remodel the RNP as it is transported or to promote release of RNA binding proteins from the mRNA in the final steps of mRNA export (Snay-Hodge *et al.*, 1998; Tseng *et al.*, 1998). It has been suggested that a function of these nucleoporins is to position Dbp5 at the NPC (Hodge *et al.*, 1999; Strahm *et al.*, 1999). Alternately, these proteins may act as docking sites for RNPs as they translocate through the NPC.

The NPC-associated protein Sac3 has been implicated previously in nuclear transport. *SAC3* was originally identified in a screen for suppressors of actin mutations (Novick *et al.*, 1989) and has been subsequently shown to be required for normal mitotic progression and spindle morphology (Bauer and Kölling, 1996b). Localizing to the NPC, Sac3 associates physically with the nucleoporin Nsp1 (Jones *et al.*, 2000). Finally, Sac3 has been ascribed a role in nuclear transport that may be related to its function in the cell cycle (Jones *et al.*, 2000).

In this study, we have characterized the role of Sac3 in mRNA export. Mutation of *SAC3* causes synthetic lethality with mutation of *MEX67*, *MTR2*, and several genes that encode cytoplasmic fibril-associated mRNA export factors. In addition, Sac3 is associated physically with Mex67, Mtr2, and other factors involved in mRNA export. By immunoelectron microscopy, Sac3 localizes exclusively to the cytoplasmic fibrils of the NPC. Finally, Mex67 accumulates at the nuclear rim in *sac3*$^-$ mutants, suggesting that Sac3 functions in the terminal step of Mex67 translocation through the NPC.

MATERIALS AND METHODS

Indirect Immunofluorescence and In Situ Hybridization

These procedures were performed as described previously (Krebber *et al.*, 1999). α-Nsp1 (gift of M. Stewart; MRC LMB, Cambridge, United Kingdom) was used at a 1:1000 dilution and detected with Texas Red-conjugated donkey α-rabbit (1.5 mg/ml; Jackson Immunoresearch Laboratories, West Grove, PA) at a 1:1000 dilution. For *sac3Δ139* and Δ*sac3-rg*, in situ hybridization was performed with a Cy3-labeled oligo dT_{50} probe at 50 nM, and all steps between probe hybridization and the first 2× SSC wash were eliminated.

Synthetic Lethal Screen

mtr2-142 cells (PSY1720) carrying a plasmid encoding pJT10-*MTR2-URA3-ADE8* (pPS1852) were subjected to ethyl methanesulfonate mutagenesis to a rate of 50% killing. We screened 15,000 colonies by the colony sectoring assay for loss of sectoring (Elledge and Davis, 1988). Candidates were selected that meet the criteria for synthetic lethality as described previously (Henry and Silver, 1996) and backcrossed to parental *mtr2-142* cells (PSY1719) three times. Linkage to *SAC3* was determined by crossing this strain to ACY276, which is marked with *HIS3* at the *SAC3* locus. A spore from this cross was further outcrossed into the S288C background by crossing twice to FY23. The resulting strain was marked with the *HIS3MX6* marker downstream of *sac3Δ139* by a method described previously (Longtine *et al.*, 1998) to create PSY2555.

Immunoprecipitation

Cells (50 ml) were grown in YPD at 25–30°C to ~2×10^7 cells/ml. All subsequent steps were performed at 4°C. Pellets were lysed in 50–100 μl of ice-cold PBSMT (2.5 mM $MgCl_2$, 3 mM KCl, 0.5% Triton X-100 in phosphate-buffered saline) plus protease inhibitors (1 mM phenylmethylsulfonyl fluoride and 2 ng/ml each of pepstatin A, leupeptin, aprotinin, antipain, benzamidine, and chymostatin) by using glass beads in a FastPrep bead beater (6.5 m/s; Savant Instruments, Holbrook, NY). After lysis, an additional 1 ml of PBSMT was added, and lysates were clarified by centrifugation at 14,000 rpm for 10 min. Protein A-Sepharose (40 μl) was washed three times in PBSMT and added to 1 mg of lysate in a total of 1 ml of PBSMT. Then 1.5 μl of affinity-purified rabbit polyclonal α-green fluorescent protein (GFP) (0.9 mg/ml) was added and incubated overnight with agitation. Beads were washed three times with 750 μl of PBSMT and once with 750 μl of Tris-EDTA, pH 8.0. Sample buffer (20 μl) was added to samples and boiled for 5 min. Immunoprecipitates (IPs) and total lysate were resolved by 7% SDS-PAGE and transferred to nitrocellulose in 10 mM CAPS (3-[cyclohexylamino]-1 propane sulfonic acid), pH 11, 1% methanol. Blots were probed with α-GFP at 1:10,000 and α-myc (9E10, 200 μg/ml; Santa Cruz Biotechnology, Santa Cruz, CA) at 1:1000.

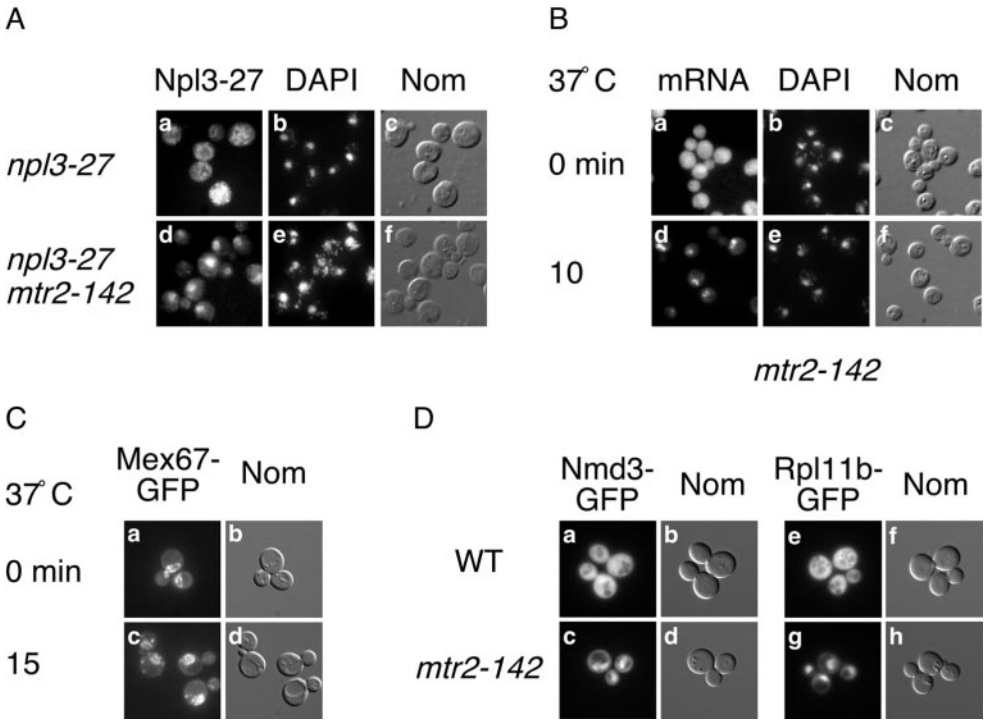

Figure 1. Characterization of the *mtr2-142* mutant. (A) *mtr2-142* causes nuclear accumulation of Npl3-27. Localization of Npl3-27 in *npl3-27* (PSY1031, a–c) and *npl3-27 mtr2-142* (PSY1717, d–f) cells. Cells were shifted to 37°C for 30 min. Indirect immunofluorescence with polyclonal antibodies to Npl3 (left), DAPI (middle), and Nomarski images (right) are shown. (B) *mtr2-142* cells display an mRNA export defect. Localization of poly $(A)^+$ RNA in *mtr2-142* cells (PSY1719) grown at 25°C (a–c) or shifted to 37°C for 10 min (d–f). In situ hybridization with an oligo $(dT)_{50}$ probe (left), DAPI (middle), and Nomarski images (right) are shown. (C) *mtr2-142* cells mislocalize Mex67 to the cytoplasm. Localization of Mex67-GFP in *mtr2-142* cells (PSY2857) grown at 25°C (a and b) or shifted to 37°C for 15 min (c and d). GFP fluorescence (left) and Nomarski images (right) are shown. (D) *mtr2-142* cells display a large ribosome export defect. Localization of Nmd3-GFP in wild-type (FY23, a and b) and *mtr2-142* cells (PSY1719, c and d). Localization of Rpl11b-GFP in wild-type (e and f) and *mtr2-142* cells (g and h). Cells were grown at 25°C.

Immunoelectron Microscopy

Spheroplasted, Triton X-100 extracted ECFP-Sac3 cells were incubated with α-GFP antibody directly conjugated to 8-nm colloidal gold and processed for preembedding labeling as described previously (Fahrenkrog *et al.*, 1998).

RESULTS

Sac3 Functions in mRNA Export

In an effort to identify genes involved in mRNA export in *S. cerevisiae*, we performed a screen for mutants that disrupt the export of the hnRNP protein Npl3 (Lei *et al.*, 2001). This screen relies on a mutant form of Npl3, Npl3-27, that is slowed for nuclear import and localizes at steady state throughout the nucleus and cytoplasm of cells as determined by indirect immunofluorescence (Figure 1A, a–c) (Krebber *et al.*, 1999). We found that mutation of the mRNA export factor *MTR2* causes nuclear accumulation of Npl3-27 (Figure 1A, d–f). In addition, this mutant is temperature sensitive for growth (our unpublished data). The lesion in *MTR2* maps to a single nucleotide mutation changing Gly142 to Asp, and this mutant is thus designated *mtr2-142*.

We further characterized the *mtr2-142* mutation in isolation from *npl3-27* to determine its effects on nuclear export. *MTR2* has been implicated in the export of mRNA as a cofactor for the export receptor Mex67 (Santos-Rosa *et al.*, 1998). We examined the localization of mRNA in *mtr2-142* cells by in situ hybridization with an oligo dT_{50} probe. In cells grown at permissive growth temperature, poly $(A)^+$ RNA localizes throughout the nucleus and cytoplasm similar to wild-type (Figure 1B, a–c) but accumulates in the nuclei of cells shifted to the nonpermissive temperature for 10 min (Figure 1B, d–f). In addition, we examined the localization of Mex67-GFP in *mtr2-142* cells. At permissive growth temperature, Mex67-GFP localizes to the nuclear rim as in wild type (Figure 1C, a and b). However, in cells shifted to the nonpermissive growth temperature for 15 min, Mex67-GFP mislocalizes to the cytoplasm in a punctate pattern (Figure 1C, c and d). On longer shifts to 37°C, *mtr2-142* cells undergo considerable lysis (our unpublished data). The extent of Mex67 mislocalization in the *mtr2-142* mutant is apparently less severe than previously published mutant alleles of *mtr2* (Santos-Rosa *et al.*, 1998). Furthermore, *mtr2-142* is unable to support growth in combination with the *mex67-5* mutation, indicating a synthetic lethal relationship (our unpublished data). Therefore, *mtr2-142* results in a rapid accumulation of mRNA in the nucleus and mislocalization of Mex67 to the cytoplasm.

Because Mtr2 also functions in the nuclear export of large ribosomal subunits, we examined the localization of large ribosomal subunits in *mtr2-142*. The *mtr2-33* mutant causes nuclear accumulation of the large ribosomal subunit but not of mRNA, suggesting that Mtr2 functions in discrete export pathways (Baβler *et al.*, 2001). Export of the large ribosomal subunit can be monitored by localization of the 60S export adapter Nmd3 (Ho *et al.*, 2000) or a large ribosomal protein such as Rpl11b (Hurt *et al.*, 1999; Stage-Zimmermann *et al.*, 2000). In wild-type cells, Nmd3-GFP and Rpl11b-GFP localize throughout the nucleus and cytoplasm (Figure 1D, a and b and e and f), whereas both Nmd3-GFP and Rpl11b are

concentrated in the nucleus in nearly one 100% of *mtr2-142* cells. These defects are apparent at the permissive growth temperature, indicating a strong inhibition of 60S export.

To determine what export factors interact genetically with Mtr2, we performed a synthetic lethal screen by the colony sectoring assay by using the *mtr2-142* mutant (our unpublished data). We obtained three mutants that are likely to be complete loss of function mutations in *MTR2*. A fourth mutant was determined to harbor a mutation in *SAC3*, which encodes a nuclear pore-associated protein (Jones *et al.*, 2000). Mapping of the genetic lesion by gap repair and sequencing revealed a mutation of a single nucleotide to cause a nonsense mutation of Trp139 to Stop thus truncating Sac3 from its wild-type length of 1301 aa. This mutant is hereby referred to as *sac3Δ139*.

Given its interaction with *mtr2-142*, we examined *sac3Δ139* cells for a defect in mRNA export. *sac3Δ139* cells have a decreased rate of growth at all temperatures tested (our unpublished data). In wild-type cells, poly $(A)^+$ RNA localizes throughout the nucleus and cytoplasm as monitored by in situ hybridization (Figure 2A, a–c). In *sac3Δ139* cells, mRNA accumulates in the nucleus (Figure 2A, d–f). Similarly, the deletion mutant Δ*sac3-rg* obtained from the Saccharomyces Gene Deletion Project (Winzeler *et al.*, 1999) displays a nuclear accumulation of mRNA (Figure 2A, j–l). In the corresponding wild-type strain for Δ*sac3-rg* mutant, poly $(A)^+$ RNA localizes throughout the nucleus and cytoplasm (Figure 2A, g–i). The mRNA export defect of *sac3Δ139* cells can be rescued by introduction of a wild-type *SAC3* plasmid (our unpublished data). Furthermore, heterozygous *sac3Δ139* diploid cells display a wild-type localization of mRNA, whereas diploids homozygous for *sac3Δ139* accumulate mRNA in the nucleus (our unpublished data). Therefore, *sac3Δ139* is a recessive loss of function mutation.

Because *mtr2-142* cells display several defects in nuclear export, we examined *sac3Δ139* cells for various nuclear export phenotypes. In wild-type cells expressing Rpl11b-GFP, the reporter localizes throughout the nucleus and cytoplasm (Figure 2B, a–b). Examination of cells after a temperature shift to 37°C to reduce the pool of ribosomes and shift back to 25°C to resume synthesis is a highly sensitive assay for large ribosome export (Hurt *et al.*, 1999; Stage-Zimmermann *et al.*, 2000). On a shift to 37°C and shift back to 25°C, the localization of Rpl11b-GFP is unchanged in wild-type cells (Figure 2B, c and d). In *sac3Δ139* cells grown at 25°C, Rpl11b-GFP localizes throughout cells similar to wild type (Figure 2B, e and f). On a shift to high temperature and shift back, <10% of cells display a mild nuclear accumulation of the reporter (Figure 2B, g and h). This slight effect is milder than that of bona fide 60S export mutants as well as some mRNA export mutants (Stage-Zimmermann *et al.*, 2000). Furthermore, the localization of Nmd3-GFP is unaffected in *sac3Δ139* mutants (our unpublished data). The export of small ribosomal subunits is also unaffected (our unpublished data) (Moy and Silver, 1999). Finally, the ability to export an artificial reporter containing the simian virus 40 nuclear localization sequence (NLS) and the protein kinase inhibitor (PKI) nuclear export sequence (NES) fused to two GFP moieties was examined in *sac3Δ139* cells. The NLS-NES-GFP reporter localizes throughout the nucleus and cytoplasm in wild-type cells (Figure 2C, a and b). In *sac3Δ139* cells grown at 25°C, the NLS-NES-GFP reporter localizes

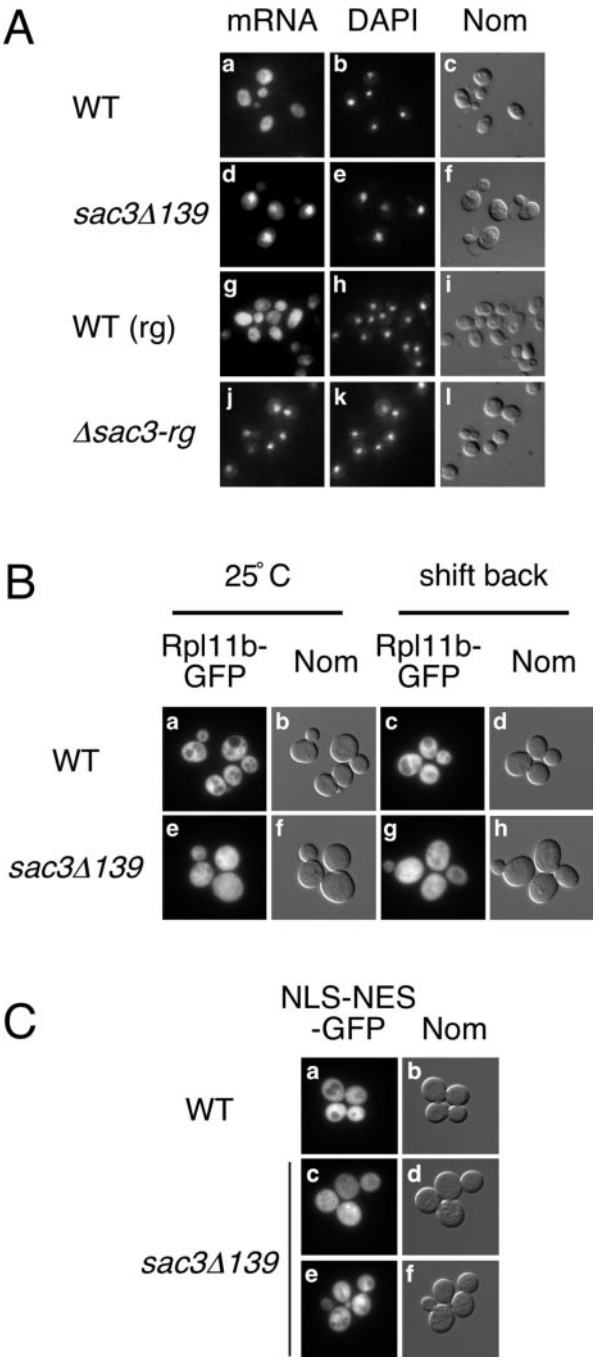

Figure 2. Sac3 functions primarily in mRNA export. A. *sac3*$^-$ mutant cells display an mRNA export defect. Localization of poly $(A)^+$ RNA in wild-type (FY23, a–c), *sac3Δ139* cells (PSY2555, d–f), wild-type (PSY1930, g–i), and Δ*sac3-rg* cells (PSY2844, j–l) grown at 30°C. In situ hybridization with an oligo $(dT)_{50}$ probe (left), DAPI (middle), and Nomarski images (right) are shown. (B) *sac3Δ139* cells do not display a large ribosome export defect. Localization of Rpl11b-GFP in wild-type (FY23, a–d) and *sac3Δ139* cells (PSY2555, e–h) grown at 25°C (a, b, e, and f) or shifted to 37°C for 1 h and back to 25°C for 1 h (c, d, g, and h). (C) *sac3Δ139* cells do not have an NES-protein export defect. Localization of NLS-NES-GFP in wild-type (FY23) and *sac3Δ139* cells (PSY2555) grown at 25°C.

Table 1. Mutations tested for synthetic lethality with *sac3Δ139*

Synthetic lethal with *sac3Δ139*	Strain	Strain reference
Yes	*mtr2-142*	This study
	mex67-5	Segref *et al.*, 1997
	rat8-2 (dbp5)	Snay-Hodge *et al.*, 1998
	rat7-1 (nup159)	Gorsch *et al.*, 1995
	nup82-Δ108[a]	Hurwitz and Blobel, 1995
No	Δ*mlp1/mlp1-Δ1*	Kölling *et al.*, 1993; Strambio-de-Castillia *et al.*, 1999
	Δ*mlp2*	Strambio-de-Castillia *et al.*, 1999
	Δ*yrb2*	Taura *et al.*, 1998
	Δ*nup116-5*	Damelin and Silver, 2003; Wente *et al.*, 1992
	gle1-L356A	Murphy and Wente, 1996

[a] This mutation resulted in a synthetic sick phenotype.

throughout the nucleus and cytoplasm in most cells (Figure 2C, c and d) although in ~15% of cells, a slight nuclear accumulation is seen (Figure 2C, e and f). When *sac3Δ139* cells are grown at 30°C or shifted to 37°C for 2 h, ~30% of cells show a slight nuclear accumulation of the NLS-NES-GFP reporter, and the same results were obtained with the Δ*sac3-rg* strain (our unpublished data). Intense nuclear accumulation of the NLS-NES-GFP reporter in the NES-protein export receptor mutant *xpo1-1* is seen in ~100% of cells when shifted to 37°C for 15 min similar to previously reported results (our unpublished data) (Stade *et al.*, 1997). Therefore, failure to export mRNA is the principal defect of *sac3Δ139* cells.

Sac3 Interacts with mRNA Export Factors

To further test the hypothesis that Sac3 is involved in mRNA export, we tested for synthetic lethality of *sac3Δ139* and various nuclear export factor mutants. This form of genetic interaction can indicate that two genes function in the same pathway or in parallel pathways. The results of these experiments are summarized in Table 1. We found that *sac3Δ139* is not synthetically lethal with deletion of the NES export factor Δ*yrb2* or factors localized to the nuclear basket, Δ*mlp1* and Δ*mlp2*. Furthermore, we found that *sac3Δ139* displays synthetic lethality with a number of mRNA export factor mutants such as *mex67-5*, *rat8-2/dbp5*, *rat7-1/nup159*, and results in synthetic sickness with *nup82-Δ108*. Interestingly, all of these factors localize predominantly to the cytoplasmic fibrils of the NPC, although Mex67 and Mtr2 localize to both the nuclear and cytoplasmic faces of the pore (Kraemer *et al.*, 1995; Hurwitz *et al.*, 1998; Santos-Rosa *et al.*, 1998; Strahm *et al.*, 1999). Two mRNA export factor mutants that *sac3Δ139* is not synthetically lethal with are Δ*nup116-5* and *gle1-L356A*. These results show that *SAC3* interacts genetically with specific mRNA export factor genes.

To assess whether Sac3 associates physically with mRNA export factors, we tested whether Sac3 could be coimmunoprecipitated from cell lysates with several export factors. Lysates were prepared from three different strains bearing a myc epitope-tagged Sac3, an EYFP-tagged Mtr2, or both tagged proteins. Western blotting with α-GFP to detect

Table 2. *S. cerevisiae* strains used in this study

Strain	Genotype	Source
FY23	MAT**a** *ura3-52 leu2Δ1 trp1Δ63*	Winston *et al.*, 1995
ACY159	MATα Δ*sac3*::*HIS3 ura3-52 leu2Δ1 his3Δ200 lys2*	Jones *et al.*, 2000
ACY276	MAT**a** *SAC3*::*SAC3-GFP-HIS3 ura3-52 leu2Δ1 his3Δ200 trp1Δ63*	This study
Dat4-2	MAT**a** *rat2-1 ura3-52 leu2Δ1 trp1Δ63*	Heath *et al.*, 1995
MEX67-GFP	MAT**a** Δ*mex67*::*HIS3 ura3 leu2 his3 trp1 ade2* ⟨pUN100 *Mex67-GFP LEU2*⟩	Santos-Rosa *et al.*, 1998
PSY1031	MATα *np13-27 ura3-52 leu2-3,112 his3 lys1-1 trp1-1 ade2-1 ade8 can1-100*	Krebber *et al.*, 1999
PSY1717	MAT**a** *np13-27 mtr2-142 ura3-52 leu2-3,112 his3 lys1-1 ade2-1 ade8 can1-100*	This study
PSY1719	MAT**a** *mtr2-142 ura3-52 leu2-3,112 his3 lys1-1 ade2-1 ade8 can1-100*	This study
PSY1720	MATα *mtr2-142 ura3-52 leu2-3,112 his3 lys1-1 ade2-1 ade8 can1-100*	This study
PSY1832	MAT**a** *NUP116*::*NUP116-EYFP-URA3 ura3-52 leu2Δ1 trp1Δ63*	Damelin and Silver, 2000
PSY2451	MAT**a** *SAC3*::*SAC3-13myc-kanMX6 ura3-52 leu2Δ1 trp1Δ63*	This study
PSY2555	MAT**a** *sac3Δ139*::*HIS3MX6 ura3 leu2 his3*	This study
PSY2691	MAT**a** *SAC3*::*SAC3-13myc-kanMX6* Δ*mex67*::*HIS3 ura3 leu2 his3 trp1 ade2* ⟨pUN100 *Mex67-GFP LEU2*⟩	This study
PSY2726	MAT**a** *DBP5*::*NOP1*$_{pro}$*-ECFP-DBP5-TRP1 ura3-52 leu2Δ1 trp1Δ63*	This study
PSY2729	MAT**a** *MTR2*::*NOP1*$_{pro}$*-EYFP-MTR2-TRP1 ura3-52 leu2Δ1 trp1Δ63*	This study
PSY2747	MAT**a** *SAC3*::*SAC3-13myc-kanMX6 MTR2*::*NOP1*$_{pro}$*-EYFP-MTR2-URA3 leu2Δ1 trp1Δ63*	This study
PSY2751	MAT**a** *MLP1*::*MLP1-EYFP-URA3 ura3-52 leu2Δ1 trp1Δ63*	This study
PSY2752	MAT**a** *MLP1*::*MLP1-EYFP-URA3 SAC3*::*SAC3-13myc-kanMX6 ura3-52 leu2Δ1 trp1Δ63*	This study
PSY2755	MAT**a** *SAC3*::*SAC3-13myc-kanMX6 DBP5*::*NOP1*$_{pro}$*-ECFP-DBP5-TRP1 ura3-52 leu2Δ1 trp1Δ63*	This study
PSY2842	MAT**a** *sac3Δ139*::*HIS3MX6* Δ*mex67*::*HIS3 ura3 leu2 his3 trp1* ⟨pUN100 *Mex67-GFP LEU2*⟩	This study
PSY2843	MATα *sac3Δ139*::*HIS3MX6* Δ*mex67*::*HIS3 ura3 leu2 his3 trp1* ⟨pUN100 *Mex67-GFP LEU2*⟩	This study
PSY2844	MAT**a** Δ*sac3*::*kanMX4 ura3Δ0 leu2Δ0 his3Δ1 met15Δ0*	Winzeler *et al.*, 1999
PSY2856	MAT**a** *SAC3*::*SAC3-13myc-kanMX6 NUP116*::*NUP116-EYFP-URA3 ura3-52 leu2Δ1 trp1Δ63*	This study
PSY2857	MATα *mtr2-142* Δ*mex67*::*HIS3 ura3 leu2 his3 lys1 trp1 ade2* ⟨pUN100 *Mex67-GFP LEU2*⟩	This study

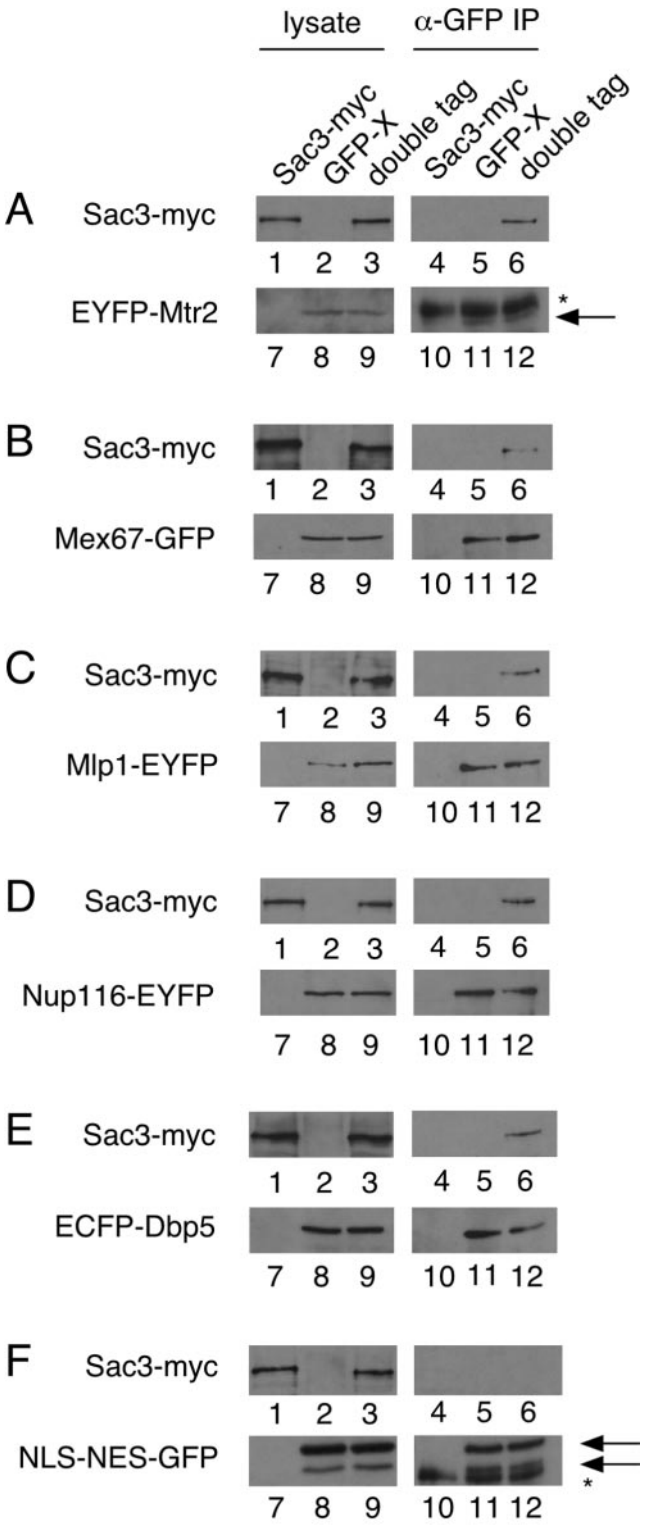

Figure 3. Sac3 associates physically with mRNA export factors and nuclear pore associated proteins. (A) Sac3 coimmunoprecipitates with Mtr2. Lysates (left) and α-GFP immunoprecipitates (right) from Sac3-myc (PSY2451, lanes 1, 4, 7, and 10), EYFP-Mtr2 (PSY2729, lanes 2, 5, 8 and 11), and double tagged Sac3-myc EYFP-Mtr2 (PSY2747, lanes 3, 6, 9 and 12) strains. The asterisk denotes the heavy chain of the α-GFP antibody. Arrows point to EYFP-Mtr2. Lanes 7–9 were exposed ten times longer than lanes 10–12. B. Sac3 coimmunoprecipitates with Mex67. Lysates (left) and α-GFP immunoprecipitates (right) from Sac3-myc (PSY2451, lanes 1, 4, 7 and 10), Mex67-GFP (lanes 2, 5, 8 and 11), and double tagged Sac3-myc Mex67-GFP (PSY2691, lanes 3, 6, 9 and 12) strains. C. Sac3 coimmunoprecipitates with Mlp1. Lysates (left) and α-GFP immunoprecipitates (right) from Sac3-myc (PSY2451, lanes 1, 4, 7, and 10), Mlp1-EYFP (PSY2751, lanes 2, 5, 8, and 11), and double-tagged Sac3-myc Mlp1-EYFP (PSY2752, lanes 3, 6, 9, and 12) strains. (D) Sac3 coimmunoprecipitates with Nup116. Lysates (left) and α-GFP immunoprecipitates (right) from Sac3-myc (PSY2451, lanes 1, 4, 7, and 10), Nup116-EYFP (PSY1832, lanes 2, 5, 8, and 11), and double-tagged Sac3-myc Nup116-EYFP (PSY2856, lanes 3, 6, 9, and 12) strains. (E) Sac3 coimmunoprecipitates with Dbp5. Lysates (left) and α-GFP immunoprecipitates (right) from Sac3-myc (PSY2451, lanes 1, 4, 7, and 10), ECFP-Dbp5 (PSY2726, lanes 2, 5, 8, and 11), and double-tagged Sac3-myc ECFP-Dbp5 (PSY2755, lanes 3, 6, 9, and 12) strains. (F) Sac3 does not coimmunoprecipitate with NLS-NES-GFP. Lysates (left) and α-GFP immunoprecipitates (right) from a Sac3-myc strain containing empty vector (PSY2451 transformed with pPS703; lanes 1, 4, 7, and 10), a wild-type strain expressing NLS-NES-GFP (FY23 transformed with pPS1372; lanes 2, 5, 8, and 11), and a Sac3-myc strain expressing NLS-NES-GFP (PSY2451 transformed with pPS1372; lanes 3, 6, 9, and 12). The asterisk denotes the heavy chain of the α-GFP antibody. Arrows point to two bands corresponding to NLS-NES-GFP. Samples were run on an SDS-PAGE gel. Lysate (10 μg) and 1/20th of the IP (from a total of 1 mg of lysate) were blotted with α-GFP (lanes 7–12) and 10 μg of lysate and the remainder of the IP were blotted with α-myc (9E10, lanes 1–6).

EYFP-Mtr2 shows expression only in the EYFP-Mtr2 and the double-tagged strains (Figure 3A, lanes 7–9). By using α-myc antibody, Sac3-myc is detectable only in the Sac3-myc and double-tagged strains (Figure 3A, lanes 1–3). Lysates from each strain were immunoprecipitated with α-GFP antibody against EYFP-Mtr2. Equal amounts of EYFP-Mtr2, which migrates just below the heavy chain of the α-GFP antibody, are immunoprecipitated from the EYFP-Mtr2 and double-tagged strains (Figure 3A, lanes 10–12). In the double-tagged strain but not single tagged strains, Sac3-myc is detectable in the immunoprecipitate (Figure 3A, lanes 4–6), indicating that Sac3 interacts physically with Mtr2. In the same manner, we examined whether Sac3 associates physically with Mex67, which interacts stably with Mtr2 (Santos-Rosa *et al.*, 1998). Western blotting of lysates from Sac3-myc, Mex67-GFP, and double-tagged strains by using α-myc and α-GFP antibodies show even levels of expression of Sac3-myc and Mex67-GFP, respectively, only in strains with the appropriate epitope tag (Figure 3B, lanes 1–3, 7–9). When lysates from Sac3-myc, Mex67-GFP, and double-tagged strains are immunoprecipitated using α-GFP antibody, which recognizes Mex67-GFP, Mex67-GFP is efficiently immunoprecipitated in the Mex67-GFP and double-tagged strains (Figure 3B, lanes 10–12). Sac3-myc is detectable in the immunoprecipitate of the double-tagged strain only, indicating that Sac3 and Mex67 can be coimmunoprecipitated (Figure 3B, lanes 4–6). Therefore, Sac3 interacts physically with the mRNA export factors Mtr2 and Mex67.

We next tested whether Sac3 interacts physically with NPC-associated proteins. It has been shown previously that

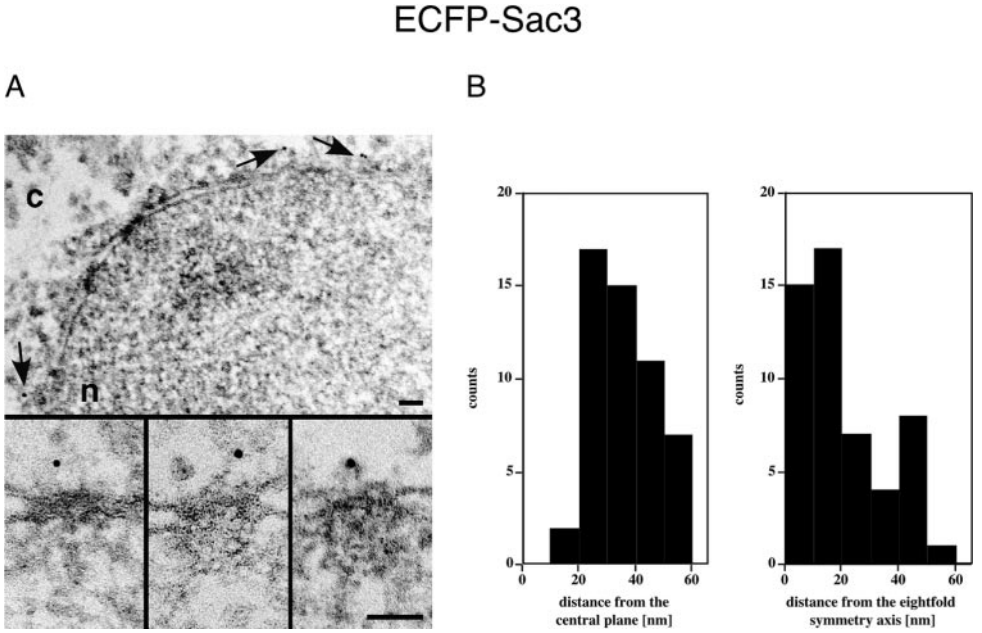

Figure 4. Immunogold-localization of Sac3 in ECFP-Sac3 cells. (A) Triton X-100–extracted spheroplasts from ECFP-Sac3 cells were preimmunolabeled with a polyclonal anti-GFP antibody directly conjugated to 8-nm colloidal gold. Shown is a view along a cross-sectioned nuclear envelope stretch with labeled NPCs (arrows, top), and a gallery of selected samples of gold-labeled NPC cross sections (bottom). The anti-GFP antibody labeled exclusively the cytoplasmic periphery of the NPC. c, cytoplasm; n, nucleus. Bars, 100 nm. (B) Quantitative analysis of the gold particles associated with the NPC. Fifty-two gold particles were scored.

Sac3 can be copurified with the nucleoporin Nsp1 from cell lysates, indicating that Sac3 associates physically with the NPC (Jones *et al*., 2000). We examined whether Sac3 could be coimmunoprecipiatated with the yeast homologue of mammalian Tpr, Mlp1, which has been shown to localize to the nuclear basket of the NPC (Strambio-de-Castillia *et al*., 1999; Kosova *et al*., 2000). When lysates from Sac3-myc, Mlp1-EYFP, and double-tagged strains are subjected to immunoprecipitation with α-GFP antibody against Mlp1-EYFP, Sac3-myc is visible in the immunoprecipitate of the double-tagged strain only, indicating that both proteins exist in a complex (Figure 3C). Interestingly, it has been stated as unpublished data that Mlp2, which is redundant with Mlp1, can be copurified with Mex67 and Mtr2 (Kosova *et al*., 2000). Furthermore, overexpression of Mlp1 causes nuclear accumulation of poly $(A)^+$ RNA, possibly implicating Mlp1 in the mRNA export process (Kosova *et al*., 2000). We also examined whether Sac3 can be coimmunoprecipitated with the nucleoporin Nup116, which is essential for proper mRNA export (Wente and Blobel, 1993). In the same manner, we tested whether α-GFP immunoprecipitation against Nup116-EYFP in Sac3-myc, Nup116-EYFP, and double-tagged strains results in copurification of Sac3-myc. Western blotting shows that Sac3-myc is detectable in the immunoprecipitation from the double-tagged strain only (Figure 3D), indicating that Sac3 associates physically with Nup116.

Finally, we tested whether Sac3 could be coimmunoprecipitated with the RNA helicase Dbp5. Dbp5 is an mRNA export factor that localizes to the cytoplasmic fibrils of the NPC (Schmitt *et al*., 1999; Strahm *et al*., 1999). Sac3-myc is detectable in the α-GFP immunoprecipitate of the double-tagged but not single-tagged Sac3-myc or ECFP-Dbp5 strains (Figure 3E). To ensure that Sac3 does not simply associate with the GFP moiety of GFP-tagged proteins, we also examined whether Sac3 interacts physically with the plasmid borne NLS-NES-GFP reporter, which continuously shuttles between the nucleus and the cytoplasm through the NPC. Western blotting of lysates from Sac3-myc cells transformed with vector, wild-type cells expressing NLS-NES-GFP, and Sac3-myc cells expressing NLS-NES-GFP shows Sac3-myc expression only in Sac3-myc cells transformed with either plasmid (Figure 3F, lanes 1–3). NLS-NES-GFP expression is visible as a doublet in wild-type and Sac3-myc cells transformed with NLS-NES-GFP plasmid (Figure 3F, lanes 7–9). In cells transformed with NLS-NES-GFP, α-GFP can immunoprecipitate NLS-NES-GFP, which migrates closely to the heavy chain of the α-GFP antibody (Figure 3F, lanes 10–12). Sac3-myc is not present in the immunoprecipitates from any of the three strains (Figure 3F, lanes 4–6), indicating that Sac3-myc does not associate with all GFP-tagged proteins. In addition, we were able to detect consistently ECFP-Dbp5, EYFP-Mtr2, and Mex67-GFP in α-myc immunoprecipitations directed against Sac3-myc in the reverse experiment (our unpublished data). These results indicate that Sac3 interacts physically with the mRNA export factors Mtr2, Mex67, and Dbp5 as well as the NPC-associated proteins Mlp1 and Nup116.

Sac3 Localizes to Cytoplasmic Fibrils of NPC

To determine the precise localization of Sac3 within the NPC, we performed immunoelectron microscopy by using epitope-tagged Sac3. Previously, it has been shown that Sac3 localizes exclusively to the nuclear rim by using a GFP-fusion (Jones *et al*., 2000). To localize Sac3, preembedding labeling immunoelectron microscopy by using a yeast strain expressing ECFP-Sac3 was carried out. An α-GFP antibody conjugated directly to 8-nm colloidal gold labeled only the cytoplasmic face of the NPC (Figure 4A). Quantitation of the gold particle distribution associated with the NPC with respect to the central plane of the nuclear envelope revealed that 95% of the gold particles were detected at distances from 20–60 nm (average dis-

tance 36.9 ± 10.5 nm) from the central plane (Figure 4B). With respect to the eightfold symmetry axis of the NPC, 95% of the gold particles were distributed over a broad range at distances from 0 to 50 nm (average distance 20.2 ± 15.3 nm) from this plane. From these results, we concluded that ECFP-Sac3 is associated exclusively with the cytoplasmic filaments of the NPC. We obtained similar results with C-terminal myc and GFP epitope tags on Sac3 (our unpublished data).

We also tested whether Sac3 localization is dependent on other transport factors. Dbp5 localizes to the nuclear rim and the cytoplasm in wild-type cells, but in *xpo1-1* cells, Dbp5 accumulates in the nucleus, suggesting that Dbp5 shuttles through the nucleus (Hodge *et al.*, 1999). We localized ECFP-Sac3 in *xpo1-1* cells by fluorescence microscopy and found its localization to be unaffected compared with wild type (our unpublished data), indicating that it does not shuttle in a *XPO1/CRM1*-dependent manner. Similarly, Sac3 localization is also unaffected in the *mtr2-142* mutant (our unpublished data).

Sac3 Is Required for Proper Localization of Mex67

To determine whether Sac3 may function in the translocation of Mex67 through the NPC, we examined the localization of Mex67 and Mtr2 in the *sac3Δ139* mutant. In wild-type cells, Mex67-GFP localizes to the nuclear rim (Figure 5A, a and b). In *sac3Δ139* cells, Mex67-GFP is localized to the entire nuclear rim as in wild type; however, a single strong focus several times the intensity of the rest of the nuclear rim is visible (Figure 5A, c and d). Western blotting was performed to verify that Mex67-GFP levels are similar in wild-type and *sac3Δ139* cells (our unpublished data). A similar and more profound defect of Mex67-GFP mislocalization was visible in *SAC3Δ* cells (ACY159) (our unpublished data). In contrast, Mtr2-GFP was unaltered in *sac3*$^-$ cells compared with wild type, suggesting that the defect of Mex67 localization in *sac3*$^-$ cells is not a result of Mtr2 mislocalization (our unpublished data). We conclude that *SAC3* is required for proper localization of Mex67.

The mislocalization of Mex67 in *sac3Δ139* cells is not due to pore clustering, a phenotype of some nucleoporin mutants. To examine the distribution of nuclear pores, we localized the nucleoporin Nsp1 in the *sac3Δ139* mutant. By indirect immunofluorescence, Nsp1 is visible as a punctate signal at the nuclear rim in wild-type cells grown at 25°C (Figure 5B, a and b). In a pore clustering mutant *rat2-1*, NPCs are clustered on one side of the nucleus (Heath *et al.*, 1995), and Nsp1 signal concentrates in a crescent shape adjacent to the DAPI signal (Figure 5B, c and d). In *sac3Δ139* cells, Nsp1 localizes to the entire nuclear rim similar to wild type (Figure 5B, e and f), indicating that NPCs do not cluster in *sac3Δ139* cells. The same results are obtained when cells are grown at 30°C or shifted to 37°C for 3 h (our unpublished data). Furthermore, Dbp5, which clusters in a pore clustering mutant (Snay-Hodge *et al.*, 1998), is not mislocalized in *sac3Δ139* cells (our unpublished data). Therefore, the mislocalization of Mex67 in *sac3Δ139* cells is not a result of pore clustering.

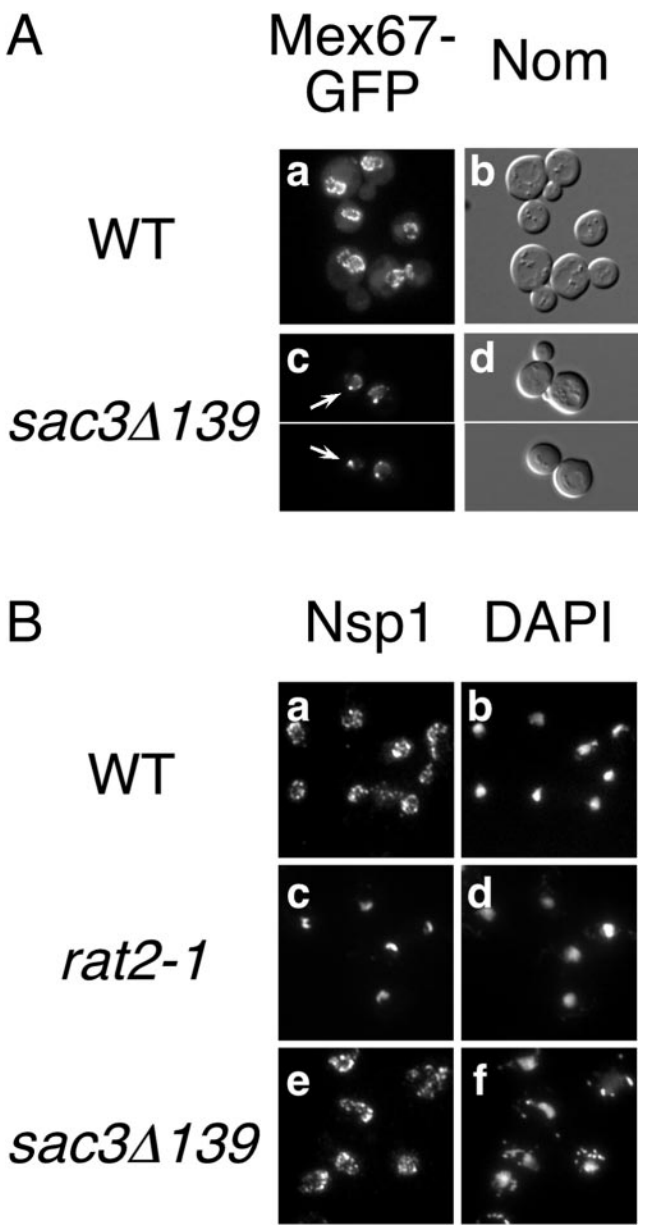

Figure 5. Mex67 mislocalizes in *sac3Δ139* cells. (A) Localization of Mex67-GFP in wild-type (MEX67-GFP, a and b) and *sac3Δ139* cells (c and d, PSY2843, top and PSY2842, bottom) grown at 30°C. GFP fluorescence (left) and Nomarski images (right) are shown. Arrows point to intense foci at the nuclear rim. (B) Localization of Nsp1 in wild-type (FY23, a and b), *rat2-1* (Dat4-2, c and d), and *sac3Δ139* cells (e and f) grown at 25°C. Indirect immunofluorescence with polyclonal antibodies to Nsp1 (left) and 4,6-diamidino-2-phenylindole (right) are shown.

DISCUSSION

Using a combination of genetic screens to identify genes involved in mRNA export, we have identified the nuclear pore-associated protein Sac3. Mutation of *SAC3* causes a

robust accumulation of mRNA in the nucleus but only mildly affects other nuclear export pathways. Furthermore, Sac3 interacts physically with several proteins involved in mRNA export and localizes exclusively to the cytoplasmic fibrils of the NPC. Finally, mutation of *SAC3* causes mislocalization of Mex67 to a strong focus at the nuclear rim. Taken together, these results show that Sac3 is involved in mRNA export and implicate Sac3 at the step of RNP translocation through the NPC.

Earlier studies have implicated Sac3 in actin function and mitotic progression. Mutations in *SAC3* were found to suppress the temperature sensitivity of the *act1-1* mutant (Novick *et al.*, 1989). A potential explanation for the suppression of *act1-1* by *sac3*$^-$ mutants is that diminished export of the defective actin transcript decreases the deleterious effects of this actin mutation. However, this possibility is unlikely because the suppression is allele specific (Bauer and Kölling, 1996a; Novick *et al.*, 1989), suggesting that loss of *SAC3* function does not bypass the *act1-1* mutation. In addition, a later study found that mutation of *SAC3* causes aberrant mitosis and spindle morphology (Bauer and Kölling, 1996b). A direct role for the actin cytoskeleton has not been established in nuclear transport, but there is speculation that RNPs may travel along cellular microfilament tracks to reach their destinations. In fact, it has been suggested that Tpr and its homologues Mlp1 and 2 may form intranuclear filaments that can serve as tracks connecting the chromatin and the NPC on which RNPs travel (Cordes *et al.*, 1997; Strambio-de-Castillia *et al.*, 1999). It is also possible that the actin cytoskeleton may be physically attached to the cytoplasmic filaments of the NPC and necessary for proper orientation of the NPC and/or the mitotic spindle. A screen for nuclear import mutants revealed that mutation of *ARP2/ACT2*, an actin-related gene, causes a defect in NPC morphology (Yan *et al.*, 1997). Currently, it is unclear as to how the nuclear transport function of Sac3 is related to its function with respect to actin.

Previously, Sac3 was ascribed a role in nuclear transport. Examination of Sac3 showed that it localizes to the nuclear rim and interacts with nucleoporins (Jones *et al.*, 2000). Specifically, Sac3 was copurified with Nsp1 from yeast lysate and was shown to interact with Nup1 and Nup159 by yeast two hybrid. Interestingly, Nsp1 and Nup159 together with Nup82 form a nucleoporin subcomplex that functions primarily in mRNA export (Belgareh *et al.*, 1998). Analysis of a *SAC3* deletion (*SAC3*Δ) strain showed synthetic lethal interactions with several NES-protein export mutants and a defect in NES-protein export (Jones *et al.*, 2000). We found that the *sac3Δ139* mutant as well an independent deletion strain (Δ*sac3-rg*) display a strong nuclear accumulation of mRNA. Consistent with our results, overexpression of *SAC3* by using a galactose-inducible promoter causes an mRNA export defect (Corbett, personal communication). In addition, in *sac3Δ139* cells no synthetic lethality with Δ*yrb2* is observed and only a mild NES-protein export defect is detected using the same reporter used in the previous study. In *SAC3*Δ cells, the NLS-NES-GFP reporter localizes exclusively to the nucleus in ~30% of cells grown at 25°C and ~50% of cells shifted to 37°C for 2 h (Corbett, personal communication). These results contrast with the mild nuclear accumulation visible in a low percentage of *sac3Δ139* and Δ*sac3-rg* cells (Figure 2C; our unpublished data). In our hands, the *SAC3*Δ strain seemed to revert to faster growing cells at a high rate, especially upon plasmid transformation (our unpublished data). Therefore, we speculate that a second mutation may be present in the *SAC3*Δ strain. Alternately, contrasting degrees of effects on NES-export in these *sac3*$^-$ mutants may be due to differences in strain background. *SAC3* as well as a number of other genes involved in mRNA export are not essential for viability. Deletion of any of several genes such as *NUP116*, *GLE2*, and *NUP133* causes profound defects in mRNA export but allows growth, although at significantly reduced rates (Wente and Blobel, 1993; Li *et al.*, 1995; Murphy *et al.*, 1996). Apparently, cells are able to compensate for lack of these genes because of the functional redundancy of various export factors.

Several findings support the notion that Sac3 functions at the translocation step of mRNA export. First, the *sac3Δ139* mutation results in synthetic lethality when combined with *mex67-5* and *mtr2-142*, both of which cause Mex67 to mislocalize to the cytoplasm upon a shift to nonpermissive temperature (Figure 1C; Segref *et al.*, 1997). The *sac3Δ139* mutant also mislocalizes Mex67; therefore, these combined mutations could further disrupt Mex67 localization and function and cause lethality. Additionally, Sac3 can be coimmunoprecipitated with Mex67, Mtr2, and Nup116 suggestive of interactions that may be required for RNP translocation through the NPC. To address whether *SAC3* may affect the interaction of Mex67 with FG-repeat–containing nucleoporins, we performed coimmunoprecipitations of Mex67 and Nup116 as described previously (Strawn *et al.*, 2001) in wild-type compared with *sac3Δ139* cells but found the interaction to be unaffected (our unpublished data). Nevertheless, Mex67 interacts with multiple FG-repeat containing nucleoporins (Sträβer *et al.*, 2000; Strawn *et al.*, 2001), and Sac3 could affect any number of these or other interactions.

More specifically, Sac3 may be involved in the terminal step of export. As determined by immunoelectron microscopy, Sac3 localizes exclusively to the cytoplasmic fibrils of the NPC, suggesting that it acts at a late stage of mRNA export. Sac3 may be a static NPC-associated protein because Sac3 localizes exclusively to the nuclear rim and remains properly localized in the *xpo1-1* mutant (Jones *et al.*, 2000; our unpublished data). However, we also found that Sac3 coimmunoprecipitates with Mlp1, which localizes to the nuclear basket by immunoelectron microscopy (Strambio-de-Castillia *et al.*, 1999; Kosova *et al.*, 2000). It is possible that either Mlp1 or Sac3 or both proteins are mobile factors despite being preferentially localized to opposite sides of the pore at steady state. Interestingly, Sac3 was not identified in a large-scale analysis of NPC proteins despite that it meets the criteria defined in this study (Rout *et al.*, 2000). The absence of Sac3 in this NPC purification may be a result of its sensitivity to proteolysis during the preparation or its transient interaction with the NPC. Our genetic analysis revealed specificity of interactions between *sac3Δ139* and mutations in genes encoding transport factors, perhaps providing a better indication of Sac3 function than our coimmunoprecipitation experiments. All of the synthetic lethal interactors identified in our analysis correspond to mRNA export factors that localize at least partially to the cytoplasmic fibrils of the NPC.

Understanding of the release of proteins from the mRNA remains elusive. A candidate for the mediator of this process is the RNA helicase Dbp5, which localizes to the cytoplasmic fibrils and the cytoplasm (Snay-Hodge *et al.*, 1998; Tseng *et al.*, 1998; Strahm *et al.*, 1999). Dbp5 can be coimmunoprecipitated with Sac3 from cell lysates. Furthermore, *sac3Δ139* is synthetically lethal with a mutant of *DBP5*, *rat8-2*, and with a mutant allele of *NUP159*, which is required for Dbp5 localization to the nuclear rim (Hodge *et al.*, 1999; Schmitt *et al.*, 1999). In addition, *sac3Δ139* combined with a mutant allele of *NUP82* results in synthetic sickness. A phenotype of *nup82-Δ108* cells is that Nup159 localization to the nuclear pore is disrupted (Hurwitz *et al.*, 1998). Each of these proteins seems to be important for proper localization of other cytoplasmic fibril-associated proteins involved in mRNA export and may function as terminal docking sites for RNPs during NPC translocation. Further studies should elucidate the mechanism of this complex process.

ACKNOWLEDGMENTS

We thank G. Blobel, D. Botstein, C. Cole, A. Corbett, E. Hurt, M. Rout, and S. Wente for sharing strains and plasmids. We are grateful to M. Stewart for α-Nsp1 antibodies. We thank A. Corbett for communicating unpublished data, M. Damelin for critical comments on the manuscript, and members of the Silver laboratory for thoughtful discussions. E.P.L. and T.M. were supported by grants from the Ryan Foundation and the National Cancer Institute. C.S. was supported by grants from the National Institutes of Health and American Cancer Society. B.F. was supported by a grant from the M.E. Müller Foundation. H.K. was supported by a grant from the Deutsche Forschungsgemeinshaft. This work was supported by grants from the National Institutes of Health and Human Frontiers Science Project (to P.A.S. and U.A.).

REFERENCES

Bachi, A., *et al*. (2000). The C-terminal domain of TAP interacts with the nuclear pore complex and promotes export of specific CTE-bearing RNA substrates. RNA *6*, 136–158.

Bailer, S.M., Siniossoglou, S., Podtelejnikov, A., Hellwig, A., Mann, M., and Hurt, E. (1998). Nup116p and nup100p are interchangeable through a conserved motif which constitutes a docking site for the mRNA transport factor gle2p. EMBO J. *17*, 1107–1119.

Baβler, J., Grandi, P., Gadal, O., Lessmann, T., Petfalski, E., Tollervey, D., Lechner, J., and Hurt, E. (2001). Identification of a 60S preribosomal particle that is closely linked to nuclear export. Mol. Cell *8*, 517–529.

Bauer, A., and Kölling, R. (1996a). Characterization of the SAC3 gene of *Saccharomyces cerevisiae*. Yeast *12*, 965–975.

Bauer, A., and Kölling, R. (1996b). The SAC3 gene encodes a nuclear protein required for normal progression of mitosis. J. Cell Sci. *109*, 1575–1583.

Belgareh, N., Snay-Hodge, C., Pasteau, F., Dagher, S., Cole, C.N., and Doye, V. (1998). Functional characterization of a Nup159p-containing nuclear pore subcomplex. Mol. Biol. Cell *9*, 3475–3492.

Cordes, V.C., Reidenbach, S., Rackwitz, H.R., and Franke, W.W. (1997). Identification of protein p270/Tpr as a constitutive component of the nuclear pore complex-attached intranuclear filaments. J. Cell Biol. *136*, 515–529.

Damelin, M., and Silver, P.A. (2000). Mapping interactions between nuclear transport factors in living cells reveals pathways through the nuclear pore complex. Mol. Cell *5*, 133–140.

Damelin, M., and Silver, P.A. (2002). In situ analysis of spatial relationships between proteins of the nuclear pore complex. Biophys. J. *83*, 3626–3636.

Elledge, S.J., and Davis, R.W. (1988). A family of versatile centromeric vectors designed for use in the sectoring-shuffle mutagenesis assay in *Saccharomyces cerevisiae*. Gene *70*, 303–312.

Fahrenkrog, B., Hurt, E.C., Aebi, U., and Pante, N. (1998). Molecular architecture of the yeast nuclear pore complex: localization of Nsp1p subcomplexes. J. Cell Biol. *143*, 577–588.

Flach, J., Bossie, M., Vogel, J., Corbett, A., Jinks, T., Willins, D.A., and Silver, P.A. (1994). A yeast RNA-binding protein shuttles between the nucleus and the cytoplasm. Mol. Cell. Biol. *14*, 8399–8407.

Fribourg, S., Braun, I.C., Izaurralde, E., and Conti, E. (2001). Structural basis for the recognition of a nucleoporin FG repeat by the NTF2-like domain of the TAP/p15 mRNA nuclear export factor. Mol. Cell *8*, 645–656.

Gorsch, L.C., Dockendorff, T.C., and Cole, C.N. (1995). A conditional allele of the novel repeat-containing yeast nucleoporin RAT7/NUP159 causes both rapid cessation of mRNA export and reversible clustering of nuclear pore complexes. J. Cell Biol. *129*, 939–955.

Heath, C.V., Copeland, C.S., Amberg, D.C., Del Priore, V., Snyder, M., and Cole, C.N. (1995). Nuclear pore complex clustering and nuclear accumulation of poly(A)+ RNA associated with mutation of the *Saccharomyces cerevisiae* RAT2/NUP120 gene. J. Cell Biol. *131*, 1677–1697.

Henry, M.F., and Silver, P.A. (1996). A novel methyltransferase (Hmt1p) modifies poly(A)+-RNA-binding proteins. Mol. Cell. Biol. *16*, 3668–3678.

Herold, A., Klymenko, T., and Izaurralde, E. (2001). NXF1/p15 heterodimers are essential for mRNA nuclear export in *Drosophila*. RNA *7*, 1768–1780.

Ho, J.H., Kallstrom, G., and Johnson, A.W. (2000). Nmd3p is a Crm1p-dependent adapter protein for nuclear export of the large ribosomal subunit. J. Cell Biol. *151*, 1057–1066.

Hodge, C.A., Colot, H.V., Stafford, P., and Cole, C.N. (1999). Rat8p/Dbp5p is a shuttling transport factor that interacts with Rat7p/Nup159p and Gle1p and suppresses the mRNA export defect of xpo1-1 cells. EMBO J. *18*, 5778–5788.

Hurt, E., Hannus, S., Schmelzl, B., Lau, D., Tollervey, D., and Simos, G. (1999). A novel in vivo assay reveals inhibition of ribosomal nuclear export in ran-cycle and nucleoporin mutants. J. Cell Biol. *144*, 389–401.

Hurt, E., Straβer, K., Segref, A., Bailer, S., Schlaich, N., Presutti, C., Tollervey, D., and Jansen, R. (2000). Mex67p mediates nuclear export of a variety of RNA polymerase II transcripts. J. Biol. Chem. *275*, 8361–8368.

Hurwitz, M.E., and Blobel, G. (1995). NUP82 is an essential yeast nucleoporin required for poly(A)+ RNA export. J. Cell Biol. *130*, 1275–1281.

Hurwitz, M.E., Strambio-de-Castillia, C., and Blobel, G. (1998). Two yeast nuclear pore complex proteins involved in mRNA export form a cytoplasmically oriented subcomplex. Proc. Natl. Acad. Sci. USA *95*, 11241–11245.

Iovine, M.K., Watkins, J.L., and Wente, S.R. (1995). The GLFG repetitive region of the nucleoporin Nup116p interacts with Kap95p, an essential yeast nuclear import factor. J. Cell Biol. *131*, 1699–1713.

Jones, A.L., Quimby, B.B., Hood, J.K., Ferrigno, P., Keshava, P.H., Silver, P.A., and Corbett, A.H. (2000). SAC3 may link nuclear pro-

tein export to cell cycle progression. Proc. Natl. Acad. Sci. USA *97*, 3224–3229.

Katahira, J., Sträβer, K., Podtelejnikov, A., Mann, M., Jung, J.U., and Hurt, E. (1999). The Mex67p-mediated nuclear mRNA export pathway is conserved from yeast to human. EMBO J. *18*, 2593–2609.

Kölling, R., Nguyen, T., Chen, E.Y., and Botstein, D. (1993). A new yeast gene with a myosin-like heptad repeat structure. Mol. Gen. Genet. *237*, 359–369.

Kosova, B., Panté, N., Rollenhagen, C., Podtelejnikov, A., Mann, M., Aebi, U., and Hurt, E. (2000). Mlp2p, a component of nuclear pore attached intranuclear filaments, associates with Nic96p. J. Biol. Chem. *275*, 343–350.

Kraemer, D.M., Strambio-de-Castillia, C., Blobel, G., and Rout, M.P. (1995). The essential yeast nucleoporin NUP159 is located on the cytoplasmic side of the nuclear pore complex and serves in karyopherin-mediated binding of transport substrate. J. Biol. Chem. *270*, 19017–19021.

Krebber, H., Taura, T., Lee, M.S., and Silver, P.A. (1999). Uncoupling of the hnRNP Npl3p from mRNAs during the stress-induced block in mRNA export. Genes Dev. *13*, 1994–2004.

Lee, M.S., Henry, M., and Silver, P.A. (1996). A protein that shuttles between the nucleus and the cytoplasm is an important mediator of RNA export. Genes Dev. *10*, 1233–1246.

Lei, E.P., Krebber, H., and Silver, P.A. (2001). Messenger RNAs are recruited for nuclear export during transcription. Genes Dev. *15*, 1771–1782.

Lei, E.P., and Silver, P.A. (2002). Protein, and RNA export from the nucleus. Dev. Cell. *2*, 261–272.

Levesque, L., Guzik, B., Guan, T., Coyle, J., Black, B.E., Rekosh, D., Hammarskjold, M.L., and Paschal, B.M. (2001). RNA export mediated by tap Involves NXT1-dependent interactions with the nuclear pore complex. J. Biol. Chem. *28*, 28.

Li, O., Heath, C.V., Amberg, D.C., Dockendorff, T.C., Copeland, C.S., Snyder, M., and Cole, C.N. (1995). Mutation or deletion of the *Saccharomyces cerevisiae* RAT3/NUP133 gene causes temperature-dependent nuclear accumulation of poly(A)+ RNA and constitutive clustering of nuclear pore complexes. Mol. Biol. Cell *6*, 401–417.

Longtine, M.S., McKenzie, A., 3rd, Demarini, D.J., Shah, N.G., Wach, A., Brachat, A., Philippsen, P., and Pringle, J.R. (1998). Additional modules for versatile and economical PCR-based gene deletion and modification in *Saccharomyces cerevisiae*. Yeast *14*, 953–961.

Moy, T.I., and Silver, P.A. (1999). Nuclear export of the small ribosomal subunit requires the ran-GTPase cycle and certain nucleoporins. Genes Dev. *13*, 2118–2133.

Murphy, R., Watkins, J.L., and Wente, S.R. (1996). GLE2, a *Saccharomyces cerevisiae* homologue of the *Schizosaccharomyces pombe* export factor RAE1, is required for nuclear pore complex structure and function. Mol. Biol. Cell *7*, 1921–1937.

Murphy, R., and Wente, S.R. (1996). An RNA-export mediator with an essential nuclear export signal. Nature *383*, 357–360.

Novick, P., Osmond, B.C., and Botstein, D. (1989). Suppressors of yeast actin mutations. Genetics *121*, 659–674.

Radu, A., Moore, M.S., and Blobel, G. (1995). The peptide repeat domain of nucleoporin Nup98 functions as a docking site in transport across the nuclear pore complex. Cell *81*, 215–222.

Rout, M.P., Aitchison, J.D., Suprapto, A., Hjertaas, K., Zhao, Y., and Chait, B.T. (2000). The yeast nuclear pore complex: composition, architecture, and transport mechanism. J. Cell Biol. *148*, 635–651.

Santos-Rosa, H., Moreno, H., Simos, G., Segref, A., Fahrenkrog, B., Panté, N., and Hurt, E. (1998). Nuclear mRNA export requires complex formation between Mex67p and Mtr2p at the nuclear pores. Mol. Cell. Biol. *18*, 6826–6838.

Schmitt, C., *et al*. (1999). Dbp5, a DEAD-box protein required for mRNA export, is recruited to the cytoplasmic fibrils of nuclear pore complex via a conserved interaction with CAN/Nup159p. EMBO J. *18*, 4332–4347.

Segref, A., Sharma, K., Doye, V., Hellwig, A., Huber, J., Luhrmann, R., and Hurt, E. (1997). Mex67p, a novel factor for nuclear mRNA export, binds to both poly(A)+ RNA and nuclear pores. EMBO J. *16*, 3256–3271.

Singleton, D.R., Chen, S., Hitomi, M., Kumagai, C., and Tartakoff, A.M. (1995). A yeast protein that bidirectionally affects nucleocytoplasmic transport. J. Cell Sci. *108*, 265–272.

Siniossoglou, S., Wimmer, C., Rieger, M., Doye, V., Tekotte, H., Weise, C., Emig, S., Segref, A., and Hurt, E.C. (1996). A novel complex of nucleoporins, which includes Sec13p and a Sec13p homolog, is essential for normal nuclear pores. Cell *84*, 265–275.

Snay-Hodge, C.A., Colot, H.V., Goldstein, A.L., and Cole, C.N. (1998). Dbp5p/Rat8p is a yeast nuclear pore-associated DEAD-box protein essential for RNA export. EMBO J. *17*, 2663–2676.

Stade, K., Ford, C.S., Guthrie, C., and Weis, K. (1997). Exportin 1 (Crm1p) is an essential nuclear export factor. Cell *90*, 1041–1050.

Stage-Zimmermann, T., Schmidt, U., and Silver, P.A. (2000). Factors affecting nuclear export of the 60S ribosomal subunit in vivo. Mol. Biol. Cell *11*, 3777–3789.

Stoffler, D., Fahrenkrog, B., and Aebi, U. (1999). The nuclear pore complex: from molecular architecture to functional dynamics. Curr. Opin. Cell Biol. *11*, 391–401.

Sträβer, K., Baβler, J., and Hurt, E. (2000). Binding of the Mex67p/Mtr2p heterodimer to FXFG, GLFG, and FG repeat nucleoporins is essential for nuclear mRNA export. J. Cell Biol. *150*, 695–706.

Sträβer, K., and Hurt, E. (2000). Yra1p, a conserved nuclear RNA-binding protein, interacts directly with Mex67p and is required for mRNA export. EMBO J. *19*, 410–420.

Strahm, Y., Fahrenkrog, B., Zenklusen, D., Rychner, E., Kantor, J., Rosbash, M., and Stutz, F. (1999). The RNA export factor Gle1p is located on the cytoplasmic fibrils of the NPC and physically interacts with the FG-nucleoporin Rip1p, the DEAD-box protein Rat8p/Dbp5p and a new protein Ymr255p. EMBO J. *18*, 5761–5777.

Strambio-de-Castillia, C., Blobel, G., and Rout, M.P. (1999). Proteins connecting the nuclear pore complex with the nuclear interior. J. Cell Biol. *144*, 839–855.

Strawn, L.A., Shen, T., and Wente, S.R. (2001). The GLFG regions of Nup116p and Nup100p serve as binding sites for both Kap95p and Mex67p at the nuclear pore complex. J. Biol. Chem. *276*, 6445–6452.

Stutz, F., Bachi, A., Doerks, T., Braun, I.C., Seraphin, B., Wilm, M., Bork, P., and Izaurralde, E. (2000). REF, an evolutionary conserved family of hnRNP-like proteins, interacts with TAP/Mex67p and participates in mRNA nuclear export. RNA *6*, 638–650.

Taura, T., Krebber, H., and Silver, P.A. (1998). A member of the Ran-binding protein family, Yrb2p, is involved in nuclear protein export. Proc. Natl. Acad. Sci. USA *95*, 7427–7432.

Teixeira, M.T., Siniossoglou, S., Podtelejnikov, S., Benichou, J.C., Mann, M., Dujon, B., Hurt, E., and Fabre, E. (1997). Two functionally distinct domains generated by in vivo cleavage of Nup145p: a novel biogenesis pathway for nucleoporins. EMBO J. *16*, 5086–5097.

Tseng, S.S., Weaver, P.L., Liu, Y., Hitomi, M., Tartakoff, A.M., and Chang, T.H. (1998). Dbp5p, a cytosolic RNA helicase, is required for poly(A)+ RNA export. EMBO J. *17*, 2651–2662.

Wente, S.R., and Blobel, G. (1993). A temperature-sensitive NUP116 null mutant forms a nuclear envelope seal over the yeast nuclear pore complex thereby blocking nucleocytoplasmic traffic. J. Cell Biol. *123*, 275–284.

Wente, S.R., Rout, M.P., and Blobel, G. (1992). A new family of yeast nuclear pore complex proteins. J. Cell Biol. *119*, 705–23.

Wiegand, H.L., Coburn, G.A., Zeng, Y., Kang, Y., Bogerd, H.P., and Cullen, B.R. (2002). Formation of Tap/NXT1 heterodimers activates Tap-dependent nuclear mRNA export by enhancing recruitment to nuclear pore complexes. Mol. Cell. Biol. *22*, 245–256.

Wilson, S.M., Datar, K.V., Paddy, M.R., Swedlow, J.R., and Swanson, M.S. (1994). Characterization of nuclear polyadenylated RNA-binding proteins in *Saccharomyces cerevisiae*. J. Cell Biol. *127*, 1173–84.

Winston, F., Dollard, C., and Ricupero-Hovasse, S.L. (1995). Construction of a set of convenient *Saccharomyces cerevisiae* strains that are isogenic to S288C. Yeast *11*, 53–55.

Winzeler, E.A., *et al*. (1999). Functional characterization of the *S. cerevisiae* genome by gene deletion and parallel analysis. Science *285*, 901–906.

Yan, C., Leibowitz, N., and Mélèse, T. (1997). A role for the divergent actin gene, ACT2, in nuclear pore structure and function. EMBO J. *16*, 3572–3586.

Zenklusen, D., Vinciguerra, P., Strahm, Y., and Stutz, F. (2001). The yeast hnRNP-Like proteins Yra1p and Yra2p participate in mRNA export through interaction with Mex67p. Mol. Cell. Biol. *21*, 4219–4232.